Sustainable Food Technology

ROYAL SOCIETY OF CHEMISTRY

PAPER

View Article Online
View Journal

Cite this: DOI: 10.1039/d5fb00752f

Mushroom mycelium as a sustainable high-protein food source: effects of submerged fermentation conditions on mycoprotein production and mycelial morphology

Krishna Kalyani Sahoo, Bruno Meireles Xavier, Mohammad Afiq Hafiy Mohammad Taufiq and Ke Wang *

Harnessing edible fungal mycelium as a source of health-promoting food presents a transformative pathway for enhancing global food security and meeting the nutritional demands of the world's growing population in the 21st century. The mycoprotein from fungal mycelium also serves as a sustainable alternative to resource-intensive animal-sourced protein. This study investigated how submerged fermentation influences the mycelial morphology and mycoprotein production of the edible fungus *Pleurotus ostreatus*. Key parameters including inoculum fragmentation, types of carbon sources, carbon-to-nitrogen (C/N) and carbon-to-phosphorus (C/P) ratios, and agitation rate were systematically evaluated. Principal component analysis (PCA) was employed to identify the most influential parameters and elucidate their correlations with production metrics. Controlled inoculum fragmentation, inoculum density and agitation were found to be crucial for achieving uniformity in pelletized mycelium and improving productivity. Protein content and production increased with a decreasing C/N ratio, achieving a maximum of 39.7% (of dry biomass) and 3.89 g L^{-1}, respectively, while they were not significantly influenced by the C/P ratio. Oleic acid, a plant-based fatty acid, was demonstrated for the first time as a sole non-sugar carbon source for *P. ostreatus* cultivation, achieving a biomass yield comparable to that of glucose. Maximum biomass production (12.9 g L^{-1}) and productivity (1.61 g L^{-1} day^{-1}) were attained under optimized inoculum fragmentation level, an inoculum density of 40 mg L^{-1}, an agitation rate of 150 rpm, a carbon loading of 3.6 g L^{-1}, a C/N ratio of 2.6 and a C/P ratio of 52.9. These findings provide valuable insights into establishing an efficient and sustainable biorefinery for mycelium-based foods.

Received 27th October 2025
Accepted 12th March 2026

DOI: 10.1039/d5fb00752f

rsc.li/susfoodtech

Sustainability spotlight

Ensuring global food security for the growing population requires sustainable, health-promoting protein sources beyond resource-intensive conventional livestock farming. Mycoprotein produced *via* submerged fermentation of edible fungi offers a promising alternative with a low carbon-footprint. This study advances the sustainable production of *Pleurotus ostreatus* mycoprotein by identifying key fermentation parameters that enhance the mycelium biomass titer and protein content while controlling the mycelial pellet morphology suitable for food applications. A significant advancement is the demonstration of oleic acid as a novel carbon source, highlighting a path towards valorizing lipid-rich feedstocks and reducing competition with food crops. This work directly supports UN SDG 2 (Zero Hunger) by enhancing mycoprotein availability and SDG 12 (Responsible Consumption and Production) by establishing efficient bioprocesses to support a circular bioeconomy.

1. Introduction

Securing a sustainable protein supply for the growing global population represents one of the most critical food security challenges.[1] A strategic transformation framework is needed towards building a more resilient and sustainable food supply to support global food security as resource-intensive livestock farming alone cannot meet the accelerating demands.[2] Mycoprotein, referring to the whole-cell, protein-rich biomass derived from fungi, stands at the forefront of this transition.[3] Cultivated from edible mycelium, it offers not only a scalable, high-quality vegan protein, containing all essential amino acids, but also provides balanced nutrition and health-promoting benefits, such as a high content of β-glucan fiber, which is known to improve gut health and help regulate blood cholesterol levels, along with other key metabolites like choline, an essential nutrient that supports liver function and brain health.[3,4] The edible fungus *Pleurotus ostreatus* is an especially promising microorganism for this purpose. Its fruiting body is

Department of Food Science, Cornell AgriTech, Cornell University, 665 W North Street, Geneva, NY, 14456, USA. E-mail: kw726@cornell.edu

well known as oyster mushroom and considered nutritious owing to the significant content of carbohydrates (43.42–66.54% biomass, dry basis (d.b.)), proteins (17.06–55.4% biomass, d.b.), and dietary fibers (7.4%3–23.63% biomass, d.b.).[5–7] *P. ostreatus* is also a good source of vitamins (*e.g.*, A, C, E and B2), minerals (*e.g.*, sodium, potassium, magnesium and calcium), and essential amino acids like lysine, phenylalanine, methionine, threonine, leucine and valine.[5,8,9] This species has been explored for the production of various bioactive compounds such as enzymes (*e.g.*, laccase and cellulase)[10,11] and exopolysaccharides (*e.g.*, β-glucans),[7] which find diverse applications in the environment and agriculture fields and food, beverage, health, pulp, textile and other industries.[12,13]

Cultivation of fungal mycelium is a sustainable approach, offering profound environmental advantages over conventional livestock farming, including substantially lower land use, water consumption, and carbon emissions.[14] By growing mycelium in efficient, controlled fermentation systems, this technology can directly meet the growing market demands for vegan proteins and novel food ingredients, decoupling food production from large-scale agriculture. Moreover, fungi can be successfully cultivated on waste substrates, such as pomelo peel powder, solid digestate from anaerobic digesters, wheat straw, tree leaves, apple peels and banana peels.[15–17] Solid-state fermentation has been widely used for fungal cultivation, mainly because of its lower energy and water requirements, cost-effectiveness, as it requires cheaper substrates, and the ability to valorize agro-industrial wastes.[18] However, this cultivation method is constrained by the requirement of a large area, inconvenient separation of mycelium biomass that is adhered to the fermented solid substrate, and challenges in maintaining a homogeneous pH, temperature and moisture-level throughout fermentation, which may potentially lead to batch-to-batch variability in the characteristics of the biomass produced.[19] In contrast, submerged fermentation is advantageous in terms of a much smaller footprint, shorter cultivation period, capability of regulating and maintaining uniform culture conditions throughout fermentation, and ease of scaling-up.[20] Furthermore, many fungi species, including *P. ostreatus*, form spherical mycelial pellets in submerged fermentation, which facilitates efficient harvesting of the mycelial biomass from the culture medium for subsequent downstream applications.[21,22] While solid-state fermentation of *P. ostreatus* has been extensively investigated for the traditional cultivation of its fruiting bodies, there are comparatively few studies on its submerged cultivation.[19,23] Submerged fermentation of *P. ostreatus* is advantageous for large-scale mycoprotein production owing to its significantly shorter production cycles (days *vs.* weeks), higher volumetric productivity, and the ability to maintain precise control over mycelial morphology and biomass composition suitable for developing food ingredients. Moreover, submerged fermentation has become an emerging area for developing mycelium-based foods, such as cultured caviar and mycoBoba from *Aspergillus awamori* (manufactured by Optimized Foods), meat analogue for Harbin red sausage by *Fusarium venenatum*,[24] oncom from *Neurospora intermedia*,[25] and dairy analogue for yogurt from *Fusarium* strain *flavolapis* (manufactured by Nature's Fynd), suggesting the need for more comprehensive research.

The type and composition of the substrate play a crucial role in determining the production of biomass and its metabolites. For instance, biomass production in submerged fermentation of *Monascus purpureus* was reported to be significantly influenced by the choice of carbon (*e.g.*, glucose, sucrose, xylose and citric acid) and nitrogen (*e.g.*, yeast leavening, NH_4Cl, peptone and soybean meal) sources.[21] Similarly, the availability of glucose and yeast extract, and supplementation of olive oil was observed to have a critical impact on protein production in *A. oryzae* and *N. intermedia*.[26] Investigating these non-sugar carbon sources (*e.g.*, fats/oil) is critical for developing more sustainable and cost-effective bioprocesses, as lipids and fatty acids can often be derived from low-cost agri-food industry byproducts, thereby avoiding competition with food crops. However, these lipids are typically used only as supplements rather than as the primary substrate; to the best of our knowledge, no studies have investigated the use of a long-chain fatty acid as the sole carbon source for submerged fungal cultivation to date. Furthermore, similar to nitrogen forming a key part of proteins, phosphorus forms a critical portion of phosphorylated biomolecules, *e.g.*, adenosine triphosphate (ATP), adenosine diphosphate (ADP) and adenosine monophosphate (AMP), and the reductant nicotinamide adenine dinucleotide phosphate (NADPH), which are essential molecules involved in energy transfer in the cells.[27] Only a few studies have explored the effect of phosphorus on the production of mycelium biomass and protein, with existing research being limited to other products such as manganese-dependent peroxidase, glucosamine and lipid in fungi species, *e.g.*, *Phanerochaete chrysosporium*, *Mucor indicus* and *Umbelopsis vinacea*.[27–29] Beyond specific nutrients, the stoichiometric relationships between carbon and nitrogen (C/N ratio) and carbon and phosphorus (C/P ratio) are critical determinants with potential influence on cell growth and metabolic pathways. Therefore, precise regulation of these ratios is indispensable for targeted modulation of metabolic fluxes, enabling the preferential allocation of cellular resources towards biomass accumulation or protein biosynthesis.[30] However, in contrast to well-studied platforms such as bacteria and microalgae, these stoichiometric relationships remain critically under-investigated in fungal submerged cultivation. Specifically, the C/N ratio has received limited attention, while the effect of the C/P ratio on biomass and protein synthesis remains entirely unexplored. Moreover, other parameters including inoculum properties (*e.g.*, inoculum density) and agitation speed have been identified as influential process conditions for mycelial growth, in addition to pellet morphology in submerged fermentation of certain species such as *Ganoderma curtisii* and *Aspergillus awamori*.[31,32] Based on the current state-of-the-art for submerged fungal fermentation, a comprehensive investigation is still required to evaluate the influence of inoculum properties, different sugar and non-sugar carbon sources, and key stoichiometric ratios (C/N and C/P) on the interplay among mycelial morphology, biomass accumulation, and protein synthesis to ultimately develop an

economically viable and environmentally sustainable process for global food security.

Therefore, to address this research gap, this study aimed at developing a robust submerged fermentation process for *Pleurotus ostreatus* to maximize the co-production of mycelial biomass and protein. The central hypothesis was that the systematic modulation of physical factors to control mycelial morphology, combined with the regulation of chemical factors to tailor nutrient availability and metabolic flux would substantially enhance both biomass titer and protein content. The objectives of this research were to: (1) evaluate the effects of key inoculum and fermentation parameters, including inoculum fragmentation level, inoculum density, and agitation rate, on mycelial pellet morphology; (2) systematically investigate the influence of medium formulation factors, including both sugar and non-sugar (such as long-chain fatty acid) as sole carbon sources and the stoichiometric C/N and C/P ratios, on the production of mycelium biomass and protein; and (3) to elucidate the complex correlations between various submerged fermentation parameters and the resulting production metrics, thereby identifying the most favorable conditions for sustainable mycoprotein production.

2. Materials and methods

2.1. Organism and culture conditions

2.1.1. Reagents and chemicals. All chemicals were of analytical grade. Glucose and fructose were procured from Ward's Science (Rochester, NY, USA). Lactose, xylose and lauric acid were procured from Thermo Fisher Scientific (Waltham, MA, USA). Magnesium sulfate and monopotassium phosphate were purchased from Ambeed Inc. (Buffalo Grove, IL, USA). Yeast extract and potato dextrose agar were purchased from Hardy Diagnostics (Santa Maria, CA, USA). Oleic acid was purchased from TCI (Portland, OR, USA). 3,5-Dinitrosalicylic acid was procured from Alfa Aesar (Ward Hill, MA, USA). Chloramphenicol was purchased from G Biosciences (Saint Louis, MO, USA). All reagents were prepared in de-ionized water.

2.1.2. Genome sequencing and species identification. As the source of fungal mycelium, oyster mushroom fruiting bodies were sourced from a local store (Ithaca, NY, USA). A 2 mm × 2 mm piece of tissue was aseptically removed from the mushroom flesh in the middle of the stem butt-end and then cultured on potato dextrose agar (PDA) for approximately 10 days.[33] The genomic DNA of the strain was extracted following a previous method[34] with minor modifications, as follows: a small fragment of mycelium was collected from a mature plate and placed into a polymerase chain reaction (PCR) tube with 50 μL of nuclease-free water. The mixture was briefly vortexed to ensure homogeneity. The tube was then incubated in a thermocycler (BIO-RAD, Model T100 Thermal Cycler, Hercules, CA, USA) for 15 min at 95 °C to facilitate cell lysis and DNA release through heat shock.[34] Following incubation, the sample was immediately cooled in an ice-water bath for 1 min to stabilize the released genomic DNA. The resulting extract was used directly as a template for PCR amplification without further mechanical or chemical treatment. PCR was carried out using ITS 5 (forward, GGA AGT AAA AGT CGT AAC AAGG, position 1737–1758) and ITS 4 (reverse, TCC TCC GCT TAT TGA TAT GC, position 2390–2409) primers (SI, Fig. S1). The amplification was performed in a 25 μL total reaction volume containing 12.5 μL of 2× master mix, 0.5 μL of forward and reverse primer each, 0.15 μL GoTaq Flexi DNA polymerase, 9.85 μL of nuclease-free water and 1.5 μL of the extracted DNA. The PCR tubes were then placed in a thermocycler and run using the appropriate conditions: initial denaturation at 95 °C for 5 min; 35 cycles of denaturation at 95 °C for 1 min, annealing at 56 °C for 1 min and extension at 72 °C for 1 min, and a final extension at 72 °C for 10 min. A 3 μL aliquot of the resulting sample was then electrophoresed on 1.5% (w/v) agarose gel. The gel was loaded with a 100 bp DNA ladder (Promega Bench Top DNA Ladder) as molecular weight markers for comparison. The gel box (InstaView Blue LED Transilluminator, Model, E1201-BLT) (Accuris Instruments, Edison, NJ, USA) was run at 120 V for 30 min until the ladder bands were appropriately separated. The gel was visualized using the gel box orange filter. Based on the primers used, we observed the sample bands appearing on the agarose gel as expected (SI, Fig. S2). The PCR sample was then cleaned using ExoSAP and subjected to Sanger sequencing at Cornell Biotechnology Resource Center (BRC) (Ithaca, NY, USA). The ITS sequences were then compared with other ITS sequences in the GenBank database using the native nucleotide Basic Local Alignment Tool (BLAST) function accessible through the National Center for Biotechnology Information (NCBI) (SI, Fig. S3 and S4), based on which the species was identified as *Pleurotus ostreatus*.

2.1.3. Media, inoculum preparation and culture conditions. The fungal mycelia were cultivated on agar plates in basal media containing (g L^{-1}): glucose (30.0), yeast extract (5.0), KH_2PO_4 (1.0), $MgSO_4$ (0.244) and agar (20.0), as previously described by Shen *et al.*[35] with minor modifications. The agar plates were incubated at 30 °C under static conditions for 6–7 days until the mycelia colonized approximately 90% of the agar surface area, as determined by the radial expansion of the mycelial front from the center of the plate. To ensure the collection of actively growing biomass, the plates were harvested before the mycelium reached the edges of the Petri dish.[35] The plates were maintained at 4 °C for further use. Inoculum preparation was performed in 300 mL shake flasks containing 150 mL of liquid basal medium (without agar). The liquid medium was inoculated with 3–4 units of 8–10 mm mycelial discs cut out from the pre-grown agar plates using sterile forceps, and the seed flasks were incubated at 30 °C and 150 rpm for 6 days in a shaker incubator (MaxQ™ 6000, Thermo Scientific, Waltham, MA, USA). The pH of the medium was adjusted to 6.0 by adding 2 M HCl or 2 M NaOH. The medium was sterilized by autoclaving at 121 °C for 15 min. The basal medium was selected based on preliminary trials (data not shown), where it supported faster mycelial growth compared to potato dextrose agar/broth to reach comparable biomass levels for inoculation.

For inoculation of the experimental flasks, 80 mL of the seed culture was transferred into a sterile 100 mL beaker containing

mainly smaller pellets of comparable sizes. The pellets were fragmented through homogenization by a mechanical homogenizer (T25 Digital Ultra-Turrax, IKA, Staufen, Germany) at 5000 rpm for 40 s. This specific fragmentation level was selected based on the study described later in Section 2.2. The resulting inoculum granulometry exhibited a mean fragment size of 924.5 μm. For all subsequent experiments, 1 mL of this homogenized pellet suspension was used as inoculum, corresponding to an inoculum density of ~20 mg L^{-1} biomass (dry basis (d.b.)) in 150 mL of liquid medium. The experimental flasks were comprised of the same basal medium as that used for inoculum generation (unless otherwise specified), except that it was supplemented with 0.1 g L^{-1} chloramphenicol to prevent microbial contamination in the submerged fermentation of fungi.[35]

2.2. Evaluation of the effect of inoculum fragmentation through homogenization

Pleurotus ostreatus was investigated for the production of biomass and morphology of pellets under varying levels of inoculum fragmentation comprised of different homogenization speeds and durations. Pre-grown seed culture was subjected to four types of fragmentation treatments following the method previously reported by Shen *et al.*,[35] with modifications based on our preliminary experimental trials (data not shown) on *P. ostreatus*, as follows: F1 (pellets homogenized at 3000 rpm for 5 s), F2 (homogenized at 5000 rpm for 10 s), F3 (homogenized at 5000 rpm for 40 s), and control (no homogenization). The pellet fragmentation was achieved using a mechanical homogenizer (T25 Digital Ultra-Turrax, IKA, Staufen, Germany). Inoculation was performed using the method mentioned earlier in Section 2.1. The cultures were incubated for 10 days under continuous shaking at 150 rpm and 30 °C.

2.3. Submerged fermentation with variable medium composition

2.3.1. Evaluation of the effect of different carbon sources and carbon loadings. Five carbon sources including glucose, lactose, fructose, xylose and oleic acid were studied as the sole carbon substrate for submerged fermentation of *P. ostreatus*. Three carbon loadings to cultivation media were investigated including 0.88, 3.60 and 6.33 g L^{-1}, corresponding to glucose concentrations of 2.19, 9.0 and 15.82 g L^{-1}, lactose concentrations of 2.08, 8.55 and 15.03 g L^{-1}, fructose concentrations of 2.19, 9.0 and 15.82 g L^{-1}, xylose concentrations of 2.19, 9.0 and 15.82 g L^{-1}, and oleic acid concentrations of 1.14, 4.71 and 8.28 g L^{-1}, respectively. Yeast extract was used as the nitrogen source for all assays at a fixed concentration (5 g L^{-1}). The cultures with different carbon loadings (0.88, 3.60 and 6.33 g L^{-1}) were incubated under constant agitation at 150 rpm and 30 °C until exhaustion of the carbon source (*e.g.*, total sugars or fatty acid) in the respective media, *i.e.*, on day 5, day 8 and day 12.

2.3.2. Evaluation of the effect of different C/N and C/P ratios. *P. ostreatus* was cultured in media containing different concentrations of nitrogen, including 0.06, 0.39, 0.72, 1.05 and 1.38 g L^{-1}, which were prepared by adding yeast extract at equivalent concentrations (0.5, 3.5, 6.5, 9.5 and 12.5 g L^{-1}, respectively). The experiment was performed using basal liquid medium containing 9 g L^{-1} glucose (and 1 g L^{-1} KH_2PO_4), which corresponded to equivalent C/N ratios of 65.5, 9.4, 5.0, 3.4 and 2.6, respectively.

Further, the organism was cultured under varying concentrations of phosphorus (0, 0.07, 0.52, 0.98 and 1.43 g L^{-1}) in the medium, which correspond to KH_2PO_4 concentrations of 0, 0.3, 2.3, 4.3 and 6.3 g L^{-1}, respectively. This study was carried out in medium containing 9 g L^{-1} glucose (and 5 g L^{-1} yeast extract), which corresponded to equivalent C/P ratios of 52.9, 6.9, 3.7 and 2.5, respectively.

The cultures were incubated for 8 days under constant agitation at 150 rpm and 30 °C.

2.4. Evaluation of the effect of different inoculum densities and agitation rates

The organism was investigated in submerged cultivation at varying inoculum densities of 20 and 40 mg L^{-1} biomass (d.b.), under different agitation rates of 75, 150 and 255 rpm at 30 °C. The cultures were grown for 8 days in media supplemented with glucose at a carbon loading of 3.6 g L^{-1}, yeast extract at a nitrogen loading of 1.38 g L^{-1} and KH_2PO_4 at a phosphorus loading of 0.07 g L^{-1}, which were selected based on the previous studies carried out in Section 2.3.

2.5. Analytical methods

2.5.1. Determination of the size distribution of inoculum fragments and pellets. The size distribution of inoculum fragments was determined using a Mastersizer particle size analyzer (MS-2000, Malvern Instruments Limited, Westborough, MA, USA) by gradually adding 30 mL sample after different fragmentation treatments. The instrument mathematically interprets the light scattering pattern by the fragments and fits the measured data to estimate a volume-based (%, v/v) particle size distribution in the range of 10–3000 μm, which is obtained as a bell-shaped plot.

For the determination of pellet sizes after submerged fermentation, 10 mL of homogenously mixed culture was poured into a Petri dish, the mycelial pellets were spread out across the dish to remove any clumps and aggregates, and discrete units of pellets visualized. Images of the Petri dish were captured inside a photo light box and the sizes of individual pellets were estimated using ImageJ software developed by the National Institutes of Health (Bethesda, MD, USA).

2.5.2. Estimation of biomass, residual sugar and fatty acid concentrations. For sampling of biomass, the experimental flask was mixed thoroughly by gentle shaking to avoid sedimentation of the mycelial pellets, and 10 mL of the culture was collected by pouring into a sterile measuring cylinder. The mycelium biomass was separated from the liquid medium *via* vacuum filtration through a pre-weighed Whatman filter paper (United Scientific, Libertyville, IL, USA), assisted by a vacuum pump (Rocker 400, Rocker Scientific, Kaohsiung City, Taiwan). The biomass residue was washed thoroughly using de-ionized

water (150 mL) for two cycles and subjected again to vacuum filtration to remove residual water and any surface-adhered medium components. The filtered and washed samples were dried at 50 °C in a convective oven (VWR Oven F Air 3.65CF, VWR International, Radnor, PA, USA) until they attained a constant weight with a change of no more than ±0.5%.[21] The moisture content of mycelium from different assays was observed to be within the range of 90.0–96.3% (SI, Table S5). The concentration of biomass in the fermentation medium was expressed as dry weight (DW) of biomass per liter of medium (g L^{-1}).

Biomass productivity was calculated according to eqn (1), as follows:

$$\text{Biomass productivity}\left(\text{g L}^{-1}\ \text{day}^{-1}\right) = \frac{\text{biomass concentration}\left(\text{g L}^{-1}\right)}{\text{fermentation period(day)}} \quad (1)$$

The initial medium and cell-free spent medium were collected and analyzed for the content of residual reducing sugar through the DNS (3,5-dinitrosalicylic acid) assay, as described earlier by Miller,[36] and measuring the absorbance using a UV-Vis spectrophotometer (UV5Bio, Mettler Toledo, Columbus, OH, USA) at 540 nm. Similarly, the cell-free supernatant was analyzed for residual concentration of fatty acid spectrophotometrically using a commercial free fatty acid assay kit (Sigma-Aldrich, St. Louis, MO, USA) and determining the absorbance at 570 nm.

Biomass yield with respect to substrate ($Y_{x/s}$) was calculated as the ratio of biomass concentration (g L^{-1}) at a given time point and the corresponding concentration of carbon source consumed according to eqn (2), as follows:

$$\text{Biomass yield}\left(\text{g g}^{-1}\right) = \frac{\text{biomass concentration}\left(\text{g L}^{-1}\right)}{\text{concentration of carbon source consumed}\left(\text{g L}^{-1}\right)} \quad (2)$$

2.5.3. Estimation of intracellular proteins. Harvested mycelium biomass initially separated from liquid media through vacuum filtration was subjected to lyophilization using a freeze-dryer with cycles of 12 h freezing and 12 h drying (EW-03336-44, Harvest Right, Salt Lake City, UT, USA). To evaluate the nutritional quality of the harvested mycelium biomass, the intracellular protein content was analyzed as previously described by Bakratsas *et al.*[23] with minor modifications. 50 mg of freeze-dried biomass was resuspended in 5 mL of phosphate buffer (pH 7.0) and subjected to ultrasonication (Q125, QSonica, Newtown, CT, USA) at 8 kHz (40% intensity) in pulse mode (15 s ON, 3 s OFF) for 6 min. The sample was placed in an ice-water bath during ultrasonication to eliminate the risk of protein degradation owing to excess heat generating from the sonication process. Intracellular contents were obtained in the supernatant by centrifuging (Centrifuge 5810 R, Eppendorf, Hamburg, Germany) the sample at 5000 rpm for 15 min. Protein content was estimated through the Bradford assay (Pierce Bradford Protein Assay Kit, Thermo Scientific, Waltham, MA, USA) using bovine serum albumin (BSA) as the standard. In brief, 1.5 mL Bradford reagent was mixed with 30 μL of cell-free supernatant and the mixture was incubated for 10 min, followed by the measurement of absorbance at 595 nm using a spectrophotometer. The absorbance value was converted into mass of proteins using the correlation based on the calibration curve ($y = 1.0404x$; $R^2 = 0.9923$), as follows:

$$\text{Concentration of protein in the sample}\left(\text{mg mL}^{-1}\right) = \frac{\text{absorbance(595 nm)}}{1.0404} \quad (3)$$

Protein content in the biomass (d.b.), protein concentration in the fermentation media, productivity and protein yield were calculated using eqn (4)–(7), respectively, as follows:

$$\text{Protein content}(\%) = \frac{\text{mass of protein(g)}}{\text{mass of biomass (d.b.)(g)}} \times 100\% \quad (4)$$

$$\text{Protein concentration (g L}^{-1}) = \text{protein content (\%)} \times \text{biomass concentration (g L}^{-1}) \quad (5)$$

$$\text{Protein productivity}\left(\text{g L}^{-1}\ \text{day}^{-1}\right) = \frac{\text{protein concentration}\left(\text{g L}^{-1}\right)}{\text{fermentation period(day)}} \quad (6)$$

$$\text{Protein yield}\left(\text{g g}^{-1}\right) = \frac{\text{protein concentration}\left(\text{g L}^{-1}\right)}{\text{concentration of carbon source consumed}\left(\text{g L}^{-1}\right)} \quad (7)$$

2.6. Statistical analysis

Experiments evaluating carbon source types and carbon loading for glucose and lactose were performed in triplicate; all other experiments were conducted in duplicate (SI, Table S3). Results were expressed as the mean ± standard deviation of the replicates. Statistical significance of the differences between the means was determined by one-way or two-way analysis of variance (ANOVA) with a post-hoc Tukey test using the OriginPro software (OriginLab, Northampton, MA, USA) at a significance level (α) of 0.05. Principal component analysis and Pearson correlation were performed using the Origin Pro software.

3. Results and discussion

3.1. Effect of inoculum fragmentation

The size of mycelium fragments in the inoculum critically influences the development of new pellets and biomass accumulation.[31] To this end, the inoculum was subjected to varying levels of fragmentation to obtain mycelium fragments of various sizes, *viz.*, control: no homogenization; F1: 3000 rpm, 5 s; F2: 5000 rpm, 10 s; and F3: 5000 rpm, 40 s. The mean sizes of mycelium fragments resulting from the different treatments including control, F1, F2 and F3 were 1110.25, 1089.13, 1036.37 and 924.5 μm, respectively. Fig. 1A shows the size distribution

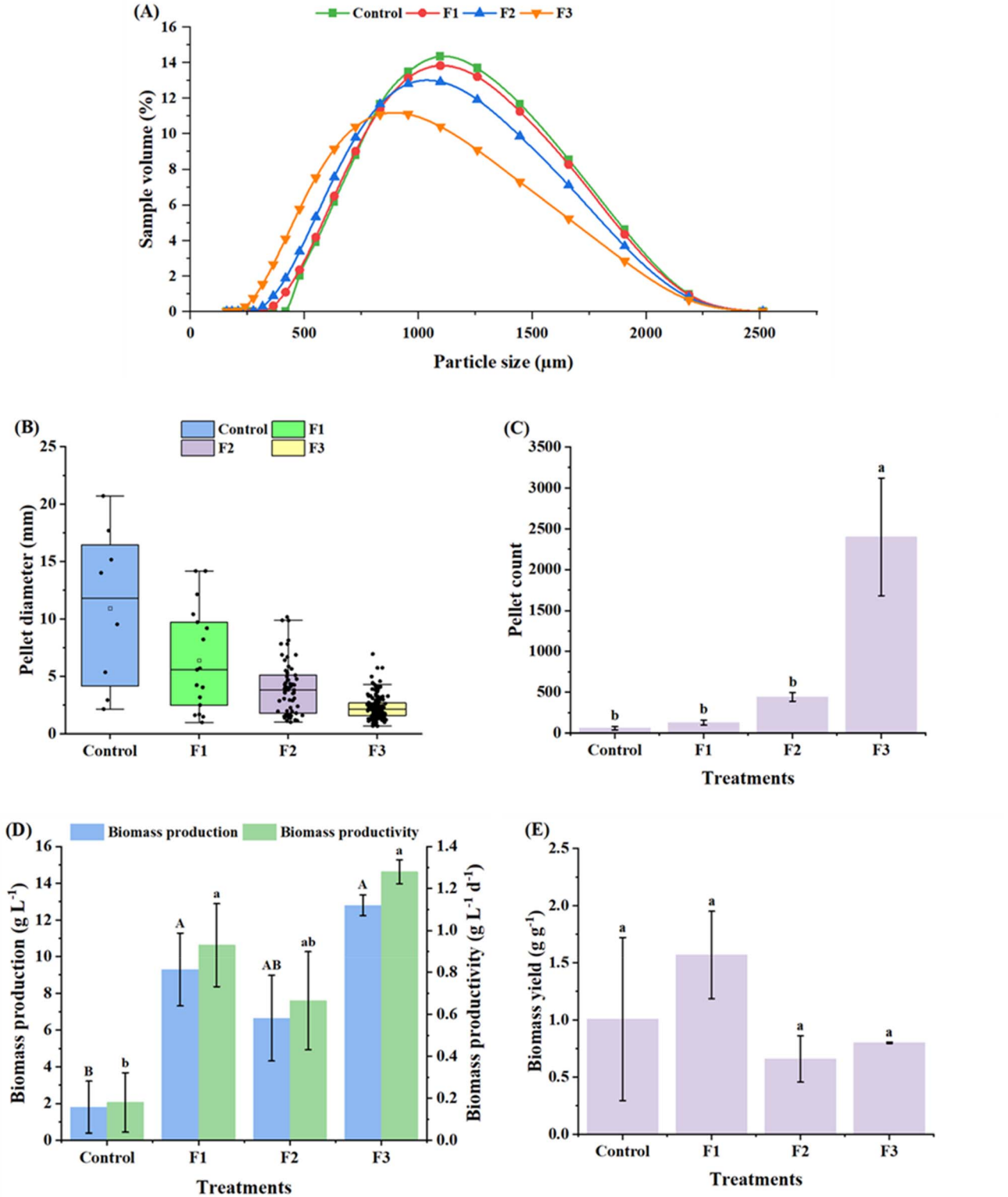

Fig. 1 Effect of different fragmentation levels on the (A) size distribution of mycelium fragments in inoculum, (B) diameter of mycelial pellets in the culture on day 10 (quartile summary of the box and whisker plots is provided in SI, Table S1), (C) number of pellets in the culture, (D) biomass production and productivity, and (E) biomass yield. Control: no homogenization; F1: 3000 rpm, 5 s; F2: 5000 rpm, 10 s; and F3: 5000 rpm, 40 s. *Groups that share the same letters are considered statistically insignificant.

of mycelium fragments in the inoculum. After fragmentation, the fraction of mycelium fragments (%, v/v of the inoculum) having sizes in the range of 1000–2500 μm was 53.9%, 51.9% and 46.3% in the control, F1 and F2 treatments, respectively. In contrast, F3, which was subjected to the highest degree of fragmentation, resulted in a major fraction (64.5%, v/v) of

fragments with a size of less than 1000 μm and only 35.5% exhibiting sizes more than 1000 μm. This fragmentation had a direct effect on the development of new pellets, which were harvested after 10 days. The pellets sizes were observed to decrease with an increasing degree of fragmentation, resulting in mean diameters of 10.9, 6.41, 3.95 and 2.26 mm from the control, F1, F2 and F3 treatments, respectively (Fig. 1B). Furthermore, with an increasing fragmentation level, the pellet size distribution became less scattered and more uniform. The control and lower fragmentation levels (F1 and F2) resulted in a lower pellet count, which did not differ significantly among the treatments ($p > 0.05$), whereas F3 exhibited a substantially higher pellet count (count: 2400) relative to the other treatments ($p < 0.05$) (Fig. 1C). As observed in Fig. 5A, while the control, F1 and F2 resulted in larger-sized mycelial pellets with spiky and rougher surfaces, F3 generated more compact pellets with relatively smoother surfaces and a more homogenous size distribution. Underdeveloped pellets were observed as numerous fine and short thread-like structures dispersed all over the medium, which were excluded from the size and count estimations. To the best of our knowledge, this is the first study demonstrating the effect of inoculum fragmentation level on the resulting pellet sizes and number in a submerged cultivation of *P. ostreatus*.

Moreover, the effect of inoculum fragmentation levels was investigated on different growth parameters, including biomass production, productivity and yield. A lower biomass titer and productivity of 1.8 g L^{-1} and 0.18 g L^{-1} day^{-1}, respectively, were observed for the control, whereas relatively higher titers (6.65–12.8 g L^{-1}) and productivities (0.66–1.28 g L^{-1} day^{-1}) were observed for F1, F2 and F3 (Fig. 1D), although the values did not vary significantly among the different fragmentation treatments ($p > 0.05$). The biomass yields across different treatments varied in the range of 0.66–1.57 g g^{-1} (Fig. 1E). These observations are in close alignment with the study reported for an *Inonotus hispidus* culture, where the biomass production was observed to increase with an increment in homogenization rate and time from 6000 to 26 000 rpm and 1 to 3 min, respectively, resulting in the maximum biomass of 10.29 g L^{-1}.[35] Moreover, Shen *et al.*[35] reported that a lower shear rate and shorter shear time yielded loose mycelial clumps and heterogeneous pellets, similar to our control, whereas a high shear rate and longer shear time produced well-dispersed evenly distributed mycelia, analogous to our F3 treatment. The dispersed morphology seems essential for creating a higher surface area per unit volume of fragmented mycelium, which can potentially enhance the uptake of nutrients and oxygen from the liquid medium, consequently leading to improved growth. Furthermore, the enhanced biomass titer and productivity under different fragmentation treatments (F1, F2 and F3) may also be attributed to the availability of a greater number of densely branched hyphal tips per unit length of an inoculum fragment, resulting in a higher germination capacity.[35] Another study also reported a similar pattern for biomass production in *Aspergillus niger* involving dispersion of the inoculum.[37] Implementation of the pellet recycling strategy revealed that fragmentation of mycelial pellets before cultivation could enhance biomass production from 27.0 g L^{-1} (1st batch) to 32.1 g L^{-1} (8th batch), whereas direct inoculation with pellets (without fragmentation) resulted in a decline in biomass production from 28.2 g L^{-1} (1st batch) to 9.2 g L^{-1} (6th batch), thus demonstrating the significance of inoculum fragmentation.[37]

In the present study, since no significant differences were observed between treatments F1, F2 and F3 in terms of biomass titer, productivity and yield (Fig. 1D and E), F3 was selected as the inoculum fragmentation level for further experiments owing to its significantly higher biomass production and productivity (compared to the control) as well as compact and relatively uniform pellet sizes (Fig. 5A).

3.2. Effect of media composition on submerged fermentation of *P. ostreatus*

3.2.1. Effect of carbon source and loading on mycelium biomass. *P. ostreatus* was cultivated with different sugar and non-sugar carbon sources including monosaccharides (glucose, fructose and xylose), a disaccharide (lactose), and a long-chain fatty acid (oleic acid) at varying carbon loadings of 0.88, 3.60 and 6.33 g L^{-1}, which were harvested on day 5, day 8 and day 12, respectively. Among the sole carbon sources, the highest mycelium biomass production and productivity were obtained using glucose. Biomass production was observed to improve with an increment in the carbon loading of glucose from 0.88–6.33 g L^{-1} (equivalent glucose concentrations: 2.19–15.82 g L^{-1}), resulting in a maximum titer of 11.2 g L^{-1} (Fig. 2A). However, the highest biomass productivity (1.09 g L^{-1} day^{-1}) was obtained at a carbon loading of 3.6 g L^{-1} (Fig. 2B). Bakratsas *et al.*[23] reported similar patterns in *P. ostreatus* biomass production, which was observed to increase from 6 to approx. 14 g L^{-1} with an increase in glucose concentration from 5 to 20 g L^{-1}. It was interesting to observe that oleic acid, as a non-sugar sole carbon source, achieved a higher biomass yield than the majority of sugar-based carbon sources in this study. A biomass production of 8.33 g L^{-1} was obtained from oleic acid at a carbon loading of 6.33 g L^{-1}, and its biomass productivity was 0.69 g L^{-1} day^{-1} at the same carbon loading, which was not significantly different from the productivity attained at a carbon loading of 3.6 g L^{-1}. Furthermore, oleic acid exhibited a higher biomass yield in the range of 1.0–1.27 g g^{-1} at different carbon loadings, which was observed to be comparable with glucose at higher loadings (3.6–6.33 g L^{-1}) (Fig. 2C).

Filamentous fungi are known to assimilate fatty acids from fats and oils within endogenous organelles, such as peroxisomes, through β-oxidation and the glyoxylate pathway, resulting in the production of carbohydrates, energy and acetyl-CoA.[38] Oleic acid is an 18-carbon unsaturated fatty acid containing 76.5% (w/w) carbon per molecule; this higher energy density possibly accounts for the higher biomass production observed in *P. ostreatus* in the present study owing to the higher energy accumulation. Oleic acid is the major fatty acid, comprising 55–83%, in olive oil.[39] Nazir *et al.*[26] demonstrated the use of olive oil (40 g L^{-1}) as the sole carbon source to grow *Aspergillus oryzae* in the presence of yeast extract, attaining a biomass titer of 13.21 g L^{-1}, which was relatively higher than the biomass

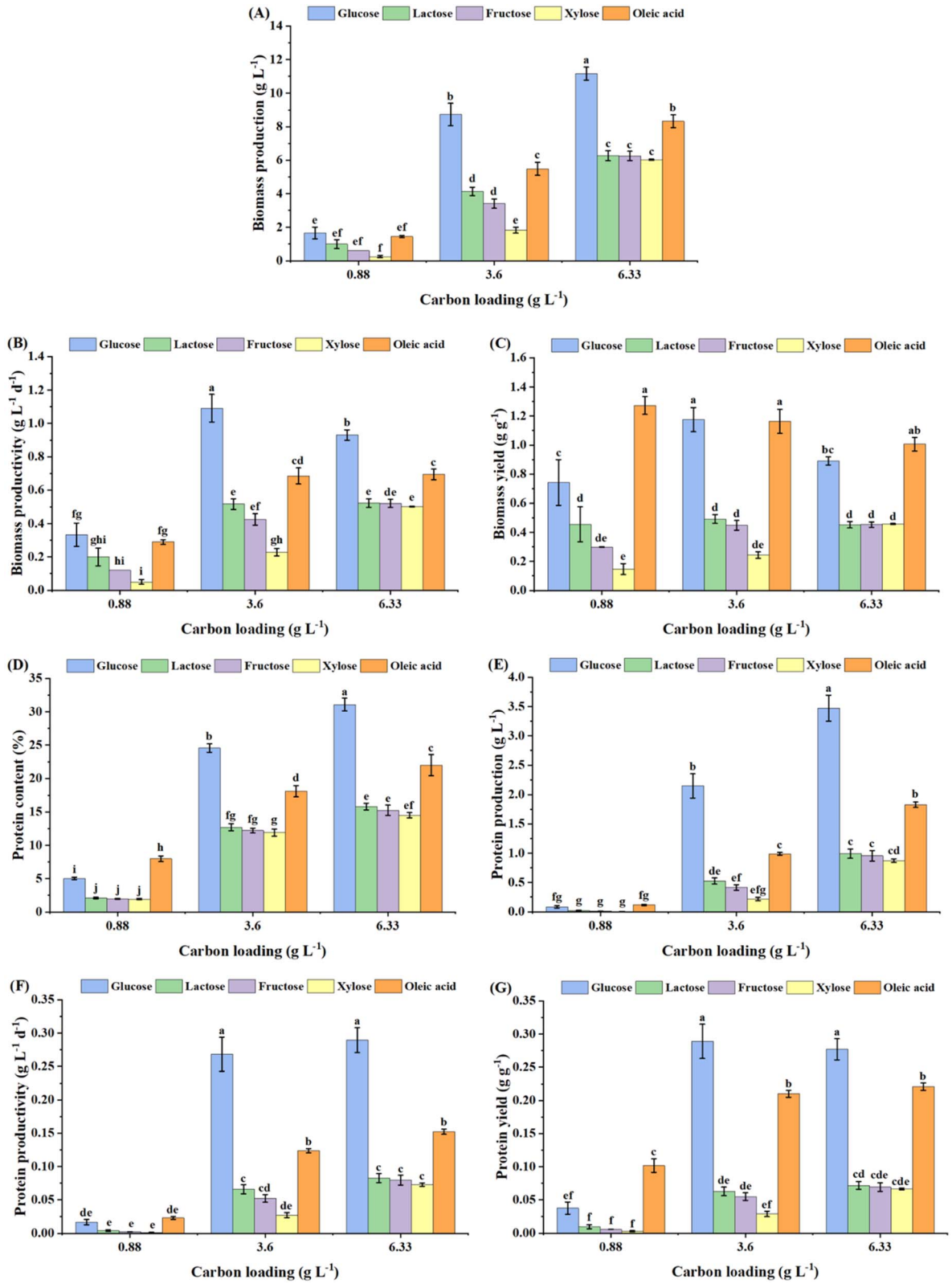

Fig. 2 Effect of different carbon loadings and carbon types on (A) biomass production, (B) biomass productivity, (C) biomass yield, (D) protein content, (E) protein production, (F) protein productivity and (G) protein yield in *Pleurotus ostreatus*. *Groups that share the same letters are considered statistically insignificant.

production (5.63 g L^{-1}) obtained using 20 g L^{-1} glucose as the sole carbon source. Moreover, researchers have demonstrated the use of olive oil as a medium supplement to enhance biomass production. For instance, Rosales-López *et al.*[31] reported that supplementation of 1% v/v olive oil in the culture medium could increase biomass production by 32% and 240% relative to optimized basal medium (containing glucose) and commercially available potato dextrose broth, respectively, in submerged fermentation of *Ganoderma curtisii*. However, to the best of our knowledge, there are no other studies demonstrating the cultivation of filamentous fungi utilizing a long-chain fatty acid as the sole carbon source. This finding is particularly significant from a sustainability standpoint, as it demonstrates the potential to valorize plant-based or lipid-rich waste streams, such as used cooking oils or agricultural byproducts, which do not compete with the arable land and food crops required for sugar-based feedstocks such as glucose and fructose. In the present study, an attempt was also made to utilize lauric acid as the carbon source under different carbon loadings (0.88–6.33 g L^{-1}). However, no growth was observed, primarily owing to its higher melting point (~43 °C), leading to a clear phase separation and flaking out of the added lauric acid as a solid layer on top of the aqueous media under the specified culture conditions (30 °C and 150 rpm). In contrast, oleic acid, could form an oil-in-water emulsion[40] under these conditions. Although the initial addition of oleic acid led to the formation of a distinct layer on the surface of the aqueous medium, this phase separation gradually diminished during the cultivation period at 150 rpm. While no external emulsifying agents were utilized, the dispersion of the fatty acid was likely facilitated by the continuous mechanical agitation in conjunction with the biological activity of the fungus. *P. ostreatus* is known to secrete extracellular lipases[41] and polysaccharides with surfactant-like properties (*e.g.*, β-glucan),[42] which can reduce the interfacial tension and promote the emulsification of lipids in submerged culture. This biological stabilization of oleic acid likely enhanced its bioavailability to the inoculum fragments for uptake and growth.

The biomass production, productivity and yield were observed to be comparable among other sugars such as lactose, fructose and xylose at the highest carbon loading of 6.33 g L^{-1}, with values significantly lower ($p < 0.05$) than that obtained with glucose and oleic acid (Fig. 2A–C, respectively). However, substantially low biomass production and productivity were observed with xylose at a carbon loading of 3.6 g L^{-1}. These results are in alignment with other studies, which have identified glucose as a superior carbon source proving higher cell biomass and product titers among other sugars. For instance, a higher production of biomass and exopolysaccharides (EPS) has been reported in *P. ostreatus* and other filamentous fungi, *e.g.*, *Inonotus hispidus*, using glucose as the carbon source, compared to other substrates, including lactose and fructose, at the same concentration.[19,35] Li *et al.*[43] justified the slower growth rate of *Neurospora crassa* on xylose through the gene expression profile of sugar transporters, deciphering that out of 39 putative sugar transporter genes in the genome of *N. crassa*, 15 and 6 genes were expressed when D-xylose and D-glucose were used as carbon sources, respectively. This suggests that glucose, being the preferred and most efficiently metabolized sugar, is handled by a small number of specialized and effective transporters. However, xylose triggers a broader, less-specialized response, upregulating a larger suite of transporters as part of a wider metabolic adjustment to a less-desirable carbon source.

3.2.2. Effect of carbon source and loading on mycelium protein. The protein content (% biomass, d.b.) and protein production from the submerged fermentation of *P. ostreatus* were observed to increase with higher carbon loadings from 0.88 to 6.33 g L^{-1}, and attained the maximum values with glucose (31.1% and 3.47 g L^{-1}), followed by oleic acid (22% and 1.83 g L^{-1}) (Fig. 2D and E), respectively. However, the protein content and production were found to be relatively lower with other carbon sources such as lactose, fructose and xylose, which could be attributed to the corresponding lower biomass yield and production from these sugars compared to glucose and oleic acid. Hamza *et al.*[19] reported a similar relationship between biomass and protein production in *Pleurotus ostreatus*, where protein production exhibited an exponential increase from day 6 to day 10, with the exponential growth of biomass following day 5 of cultivation. Furthermore, Bakratsas *et al.*[23] demonstrated a significantly higher protein content and production in *P. ostreatus* biomass cultivated using glucose (29.0% ± 2.0% and 3.32 ± 0.20 g L^{-1}) compared to lactose, fructose and xylose on day 8 of cultivation, which is well in accordance with the findings of the present study. The protein content and production from oleic acid were 7.99–21.98% and 0.12–1.83 g L^{-1}, respectively, under carbon loadings from 0.88 to 6.33 g L^{-1}, which were significantly higher than that with the majority of sugar substrates, but lower than glucose. This could be attributed to the possible metabolic switch in the cells, resulting in the diversion of energy from fatty acids towards the accumulation of fat in the cells, as a priority over synthesis of proteins. This is corroborated by Nazir *et al.*,[26] wherein, *A. oryzae* biomass accumulated 14% protein and 34% fat from 40 g L^{-1} olive oil, while it produced 48% protein and 3% fat from 20 g L^{-1} glucose. Similarly, protein productivity and protein yield from glucose were observed to attain maximum values of 0.29 g L^{-1} day^{-1} and 0.30 g g^{-1}, which were significantly higher than that from oleic acid (0.15 g L^{-1} day^{-1} and 0.22 g g^{-1}) (Fig. 2F and G) and other sugars, respectively.

Overall, the superior performance of protein production by *P. ostreatus* in the presence of glucose, followed by oleic acid, and relatively lower performance in the presence of other sources, *e.g.*, lactose, fructose and xylose, could be attributed to the poor efficiency of assimilation of these sugars into the cells compared to glucose and oleic acid. As the maximum biomass productivity and protein yield were observed with glucose at a carbon loading of 3.6 g L^{-1} (culture period: 8 days), these conditions were selected for performing further experiments, considering the industrial viability of the process. Fig. 5B shows the morphology of the pellets grown using different carbon sources at a loading of 3.6 g L^{-1}. Glucose and lactose were observed to produce several round pellets with a relatively uniform size distribution compared to fructose and xylose, which yielded the majority of pellets with rough and spiky

surfaces and a non-uniform size distribution. The pellets generated from the oleic acid-containing medium had interesting morphological features, which were prominently distinguishable from the ones yielded from sugar substrates. For instance, oleic acid yielded a greater number of compact pellets with even smoother surfaces and a more homogenous size distribution compared to the rest of the carbon sources, including glucose and lactose. The enhanced pellet morphology (compact, smooth, and uniform) observed with oleic acid suggests the potential role of lipids in modulating mycelial aggregation and morphology. This aligns with Cheng *et al.*,[44] who improved *Pleurotus* sp. pellet compaction and circularity using olive oil (containing oleic acid) combined with the surfactant Tween 80 (a synthetic source of oleic acid). Cheng *et al.*[44] speculated that Tween 80 might assist in olive oil emulsification, implying that the lipid phase influences pellet formation. Observations from our study indicate that oleic acid alone may promote similar characteristics, possibly by altering hyphal surface interactions due to its hydrophobicity, thus mimicking surfactant effects. Alternatively, this could be attributed to the potential of *P. ostreatus* to secrete extracellular lipases[41] and polysaccharides with surfactant-like properties (*e.g.*, β-glucan),[42] facilitating the emulsification of oleic acid. Although the exact mechanism warrants further investigation, these findings underscore the significant impact of lipid-based carbon sources on fungal pellet morphology.

3.2.3. Effect of C/N and C/P ratios on mycelium biomass. *P. ostreatus* was cultivated under different C/N ratios of 65.5, 9.4, 5.0, 3.4 and 2.6, which were achieved by varying the nitrogen loading in the media to 0.06, 0.39, 0.72, 1.05 and 1.38 g L^{-1}, respectively, at a fixed carbon loading. Biomass production and productivity were observed to increase significantly with an increment in nitrogen loading and decrement in C/N ratio (Fig. 3A), attaining the highest values of 9.8 g L^{-1} and 1.23 g L^{-1} day^{-1}, respectively, at an N-loading of 1.38 g L^{-1} (C/N = 2.6). These trends are in agreement with the findings of Bakratsas *et al.*,[23] where an increasing production of *P. ostreatus* biomass was achieved with an increase in the concentration of yeast extract from 5 to 15 g L^{-1}, which can be indirectly attributed to the increase in nitrogen loading. The biomass yield was remarkably low (0.4 g g^{-1}) at the lowest nitrogen loading (highest C/N ratio, *i.e.*, 65.5); however, comparable yields in the range of 0.88–1.09 g g^{-1} were obtained with a further increment in nitrogen loading from 0.39 to 1.38 g L^{-1} (Fig. 3B). Cao *et al.*[32] reported similar observations in *Aspergillus awamori*, wherein a high C/N ratio of 153 (control) resulted in the lowest production (∼5 g L^{-1}) and yield (∼0.5 g g^{-1}) of biomass; however, a reduction in the C/N ratio to 15 led to a substantial increment in these values (14.00 g L^{-1} and 0.98 g g^{-1}, respectively) relative to the control.

The improved growth metrics achieved at lower C/N ratios could be attributed to the higher nitrogen concentration in the medium, which is critical for the endogenous production of nucleotides, amino acids and other supporting cofactors. Increased availability of easily assimilated organic nitrogen sources (like those in yeast extract) directly fuels pathways such as the glutamine synthetase cycle, boosting the production of amino acids needed for protein synthesis and overall cell structure.[45] Simultaneously, ample nitrogen ensures the production of purine and pyrimidine bases for nucleotide synthesis, supporting DNA replication and RNA production required for cell division and growth.[30] Furthermore, many essential enzymatic cofactors (*e.g.*, nicotinamide adenine dinucleotide and flavin adenine dinucleotide) also contain nitrogen atoms. With a preferable carbon substrate such as glucose providing energy and carbon skeletons, abundant nitrogen allows these precursors to be readily assimilated into biomass, resulting in higher biomass titers. Conversely, a high C/N ratio leads to faster nitrogen depletion, and subsequent nitrogen starvation causes earlier transition of the fungi into stationary phase, resulting in a reduction in biomass growth and yield.[32]

In the next step, *P. ostreatus* was evaluated under varying C/P ratios of 52.9, 6.9, 3.7 and 2.5, which were obtained by supplementing different loadings of phosphorus in the medium, *viz.*, 0.07, 0.52, 0.98 and 1.43 g L^{-1} (corresponding to KH_2PO_4 concentrations of 0.3, 2.3, 4.3 and 6.3 g L^{-1}, respectively), in addition to the control unit without phosphorus (0 g L^{-1}). The highest biomass production (4 g L^{-1}) and productivity (0.5 g L^{-1} day^{-1}) were achieved at the highest C/P ratio of 52.9 (corresponding to a phosphorus loading of 0.07 g L^{-1}), which were significantly higher than that of the control ($p < 0.05$), but comparable with the performance at lower C/P ratios or higher phosphorus loadings (Fig. 3D). The biomass yield was obtained in the range of 0.9–1.04 g L^{-1} day^{-1}, clearly demonstrating that the variation in phosphorus loading did not have any impact on the yield (Fig. 3E). Liang *et al.*[28] reported a similar pattern in *Phanerochaete chrysosporium* involving an increase in biomass titer from 0.002 to 2.006 g L^{-1} with an initial increase in KH_2PO_4 concentration from 0 to 0.05 g L^{-1}; however, a further increment in the KH_2PO_4 loading (0.5–4.0 g L^{-1}) led to a reduced growth rate, producing only 2.397–2.678 g L^{-1} of biomass, which was not significantly different from the biomass titer attained at a lower KH_2PO_4 loading of 0.05 g L^{-1}. Hence, it can be inferred that although the availability of phosphorus is critical for boosting the growth of fungi, excess phosphorus beyond a certain threshold does not have a substantial impact on biomass production.

3.2.4. Effect of C/N and C/P ratios on mycelium protein. Similarly, an increase in nitrogen loading and corresponding reduction in C/N ratio (from 65.5 to 2.6) led to a significant increase in protein content from 1.84% to 39.7% and equivalent protein production from 0.01 to 3.89 g L^{-1} (Fig. 3C). There is a lack of studies delving into the effect of C/N ratio on protein production in submerged fermentation of filamentous fungi. However, the effect is well-studied in other proteinaceous cell factories. For instance, the microalga *Chlorella vulgaris* exhibited a similar pattern, showing an enhancement in protein content from 27.61% to 61.56% with a decrease in the C/N ratio from 32 : 1 to 12 : 1, which was primarily attributed to the higher availability of nitrogen to the intracellular protein synthesis machinery at a lower C/N ratio.[46] Likewise, as the C/N ratio declined from 50 to 24, single-cell protein production was observed to increase from 3.7 to 8.4 g L^{-1} in the red yeast

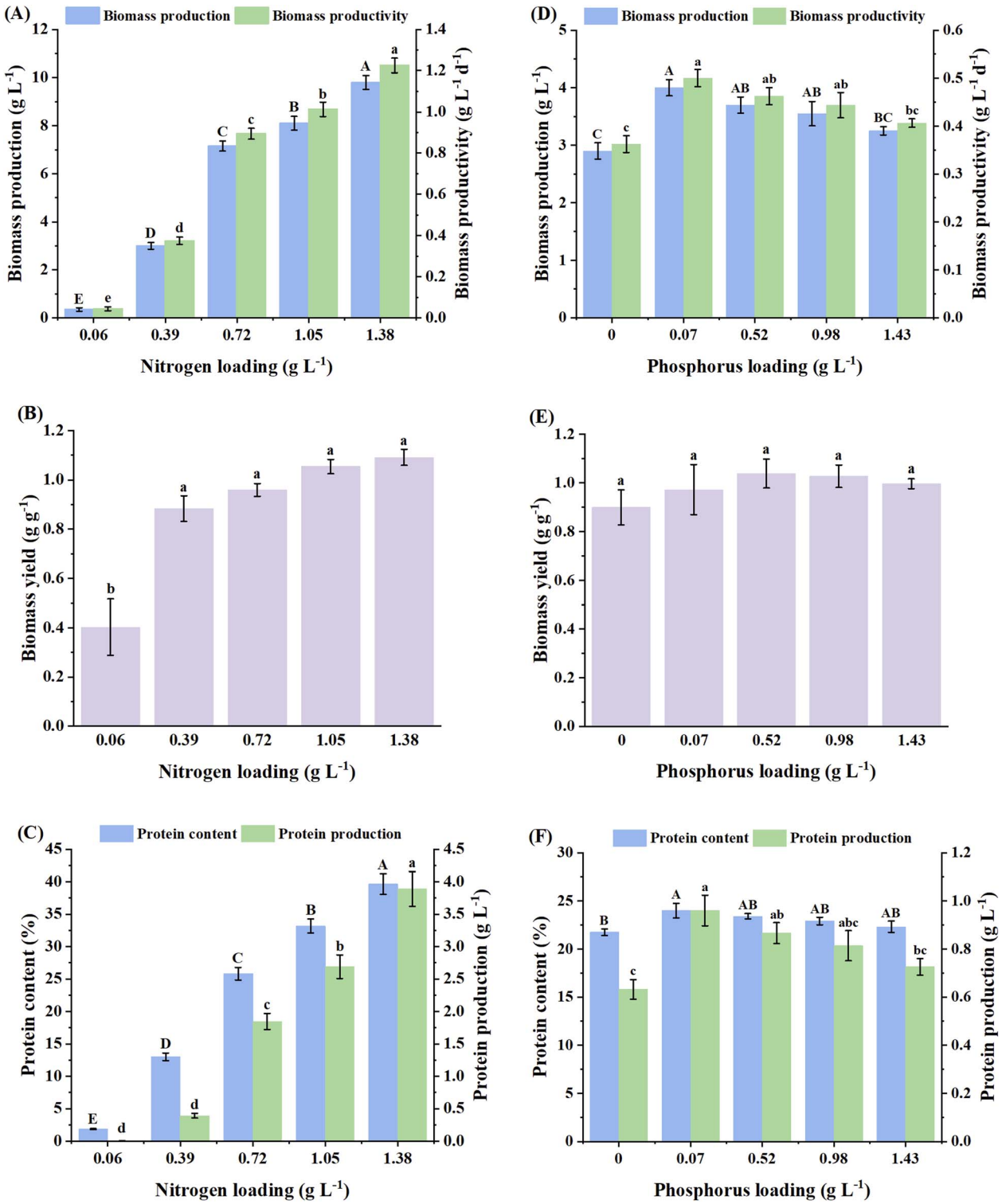

Fig. 3 Effect of varying nitrogen loadings on (A) biomass production and productivity, (B) biomass yield, and (C) protein content and protein production in *Pleurotus ostreatus*. Different nitrogen loadings (0.06–1.38 g L^{-1}) correspond to the equivalent C/N ratios of 65.5, 9.4, 5.0, 3.4 and 2.6, respectively. Effect of varying phosphorus loadings on (D) biomass production and productivity, (E) biomass yield, and (F) protein content and protein production in *Pleurotus ostreatus*. Different phosphorus loadings (0.07–1.43 g L^{-1}) correspond to the equivalent C/P ratios of 52.9, 6.9, 3.7 and 2.5, respectively. *Groups that share the same letters are considered statistically insignificant.

Sporidiobolus pararoseus.[47] A lower C/N ratio, which is associated with a higher availability of nitrogen, stimulates the cells to build more proteins primarily to support cell growth,[47] possibly explaining the higher protein content associated with higher biomass production in the present study. Moreover, the highest protein content attained in the present study (39.7%) aligns well

with the range (42.8–44.0%) reported for *Pleurotus ostreatus* cultivated using synthetic media as well waste substrates, *e.g.*, wine lees and fibre sludge-derived cellulosic hydrolysate.[10,23]

The maximum protein content (24.0%) and protein production (0.96 g L^{-1}), achieved at a phosphorus loading of 0.07 g L^{-1} (equivalent C/P ratio of 52.9), exhibited increments of 10.2% and 52.1%, respectively, relative to the control without phosphorus (Fig. 3F). However, a further increase in phosphorus loading did not cause any significant changes in the protein content and production. Similar observations were reported in *Mucor indicus*, where a variation in KH_2PO_4 concentration between 0 and 7.5 g L^{-1} did not cause any significant changes in the protein content, which was secreted within a range of 505 to 520 g kg^{-1} biomass under different conditions.[29] In the present study, the plateauing of biomass production at higher phosphorus loadings beyond 0.07 g L^{-1} could be attributed to feedback inhibition, implying that at 0.07 g L^{-1}, the fungal cells were able to fill their internal phosphorus reservoirs (*e.g.*, ATP and polyphosphate granules), thereby signaling the transporters to slow down or stop importing more phosphorus.[48] Beyond this concentration, even with abundant external phosphorus, the regulatory systems of the cell might stop taking it up, thus plateauing the growth. Furthermore, since the accumulation of protein is associated with growth, as previously reported for other species, *e.g.*, *Chlorella pyrenoidosa*,[49] likewise in the present study, a saturation in protein content and production was observed with the plateauing of biomass production beyond a phosphorus loading of 0.07 g L^{-1}.

To the best of our knowledge, this is the first study demonstrating the effect of C/P ratio on the production of biomass and protein in the submerged fermentation of filamentous fungi. However, the effects of C/P ratio observed in the present study are comparable with the outcomes in other studies concerning non-fungi-based cell systems. For instance, a variation in the C/P ratio between 282 and 474 did not cause a significant change in biomass production, showing saturation within a range of 48.1–48.9 g L^{-1} in the yeast *Sporidiobolus pararoseus*.[47] Based on the present findings, a nitrogen loading of 1.38 g L^{-1} and a phosphorus loading of 0.07 g L^{-1}, corresponding to C/N and C/P ratios of 2.6 and 52.9, respectively, were selected for further experiments. A variation in the C/N and C/P ratios did not have a significant impact on the morphology of the mycelial pellets in terms of size distribution pattern and external appearance of their surface (data not shown). In general, these pellets exhibited the same morphological attributes as those cultured using glucose at a carbon loading of 3.6 g L^{-1} (Fig. 5(i)). This implies that the pellet morphology remains consistent under fixed sources of carbon and nitrogen, unless other fermentation parameters are altered (*e.g.*, inoculum fragmentation, inoculum density and agitation).

3.3. Effect of inoculum density and agitation rate

Inoculum density and agitation rate were observed to have significant effects on the growth and morphology of the pellets in terms of size and number. Biomass production, productivity and yield were observed to increase with an increase in inoculum density from 20 to 40 mg L^{-1} under different agitation rates (Fig. 4–C), respectively. Although these growth parameters exhibited a significant improvement with an increase in the agitation rate from 75 to 150 rpm, a further increment in the agitation rate to 225 rpm resulted in a substantial decline in biomass growth in terms of titer, productivity and yield (Fig. 4A–C), respectively. Cao *et al.*[32] reported similar observations in an *Aspergillus awamori* culture, where the maximum biomass concentration was attained at 150 rpm; however, the production was observed to decline under both lower (50 rpm) and higher (250 rpm) agitation rates. The decline in biomass growth at a higher agitation rate was attributed to the fragmentation of pellets induced by high hydrodynamic shear. The broken pellets subsequently attempt to restructure into new pellets; the underlying process consumes energy, thereby diverting it from active biomass formation, resulting in a decline in growth.[32] In the present study, the highest biomass production (12.9 g L^{-1}), productivity (1.61 g L^{-1} day^{-1}) and yield (1.43 g g^{-1}) were attained using an inoculum density of 40 mg L^{-1} at 150 rpm, which were 23.4%, 23.4% and 23.1% higher than the values at a lower inoculum density (20 mg L^{-1}) under the same agitation rate, respectively. These observations are in agreement with the study reported by Shen *et al.*,[35] where biomass production was observed to increase with an increment in the inoculum density (from 8 to 40 mg L^{-1}), resulting in the maximum titer of 10.22 g L^{-1} at an inoculum concentration of 40 mg L^{-1} in *Inonotus hispidus* fermentation.

The lowest agitation rate of 75 rpm resulted in single, large-sized mycelial pellets with average sizes of 63.8 mm and 72.7 mm at inoculum densities of 20 and 40 mg L^{-1}, respectively (Fig. 5C). Fig. 5C shows the morphology of the pellets harvested on day 8. The pellet sizes decreased and the pellet count increased significantly with an increase in the agitation rate to 150 rpm. In contrast, a further increment in the agitation rate (from 150 to 225 rpm) did not result in a significant difference in the size or the number of the pellets under specific inoculum densities (Fig. 4D and E and 5C). The average pellet sizes obtained at 150 rpm were 2.02 mm (20 mg L^{-1}), 1.85 mm (40 mg L^{-1}), and at 225 rpm were 1.83 mm (20 mg L^{-1}) and 1.66 mm (40 mg L^{-1}), as shown in the box and whisker plot in Fig. 4D. A few other studies reported similar observations in terms of reduction in pellet size with an increase in agitation rate. For instance, the average pellet diameter of *Neurospora intermedia* was observed to decrease from 6.54 $\pm$ 0.62 mm to 1.92 $\pm$ 0.33 mm with an increase in the agitation rate from 100 to 150 rpm.[22] Although the inoculum density did not have a remarkable effect on the size of the pellets at higher agitation rates (150–225 rpm), the pellet number was observed to increase significantly ($p < 0.05$) with an increase in the inoculum density at the highest agitation rate of 225 rpm, *i.e.*, 705 pellets at 20 mg L^{-1} to 1154 pellets at 40 mg L^{-1} (Fig. 4D and E).

From a technological perspective, controlling the *P. ostreatus* pellet morphology *via* inoculum fragmentation, inoculum density, agitation, and media formulation can profoundly impact industrial downstream processing. In the present study, the compact, uniform pellets, achieved using fragmentation level F3, inoculum density of 20 mg L^{-1}, and agitation rate of 150 rpm, are significantly more advantageous for industrial-

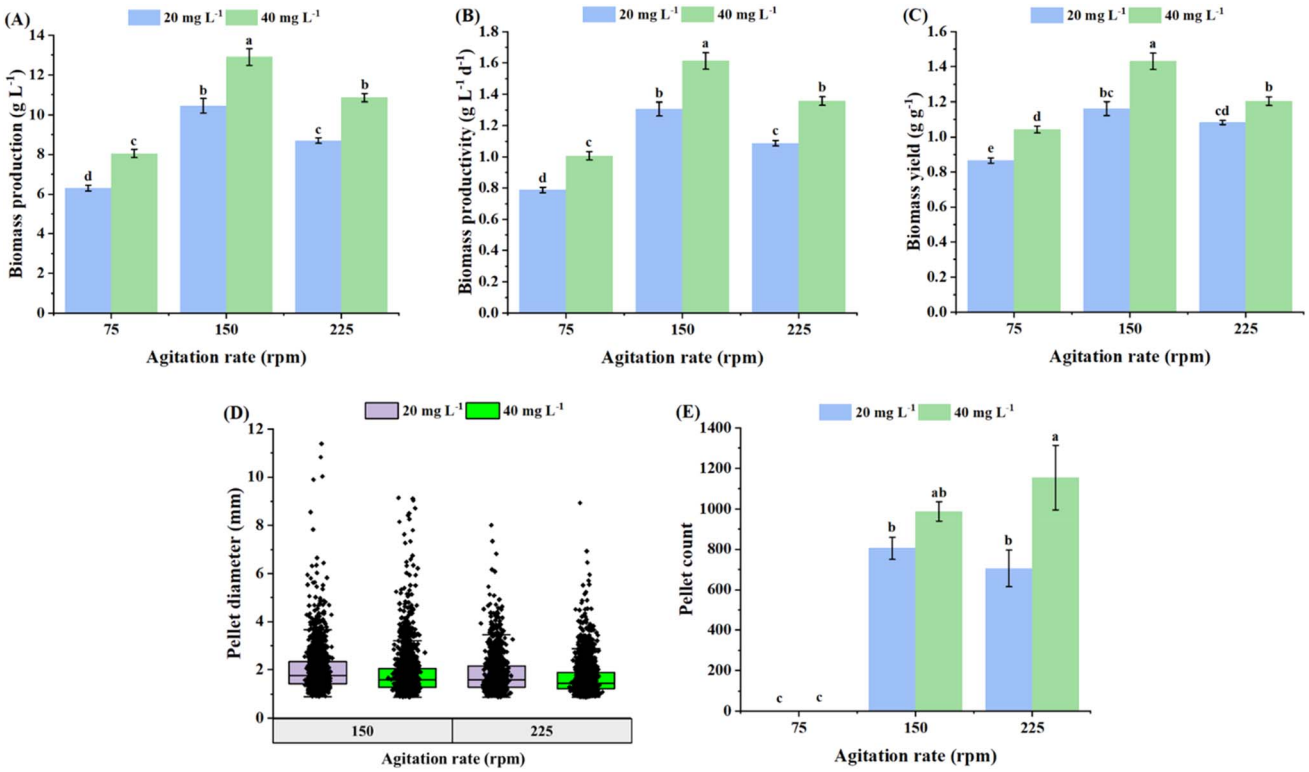

Fig. 4 Effect of different agitation rates and inoculum densities on (A) biomass production, (B) biomass productivity, (C) biomass yield, and (D) diameter of mycelial pellets on day 8 (quartile summary of the box and whisker plots is provided in SI, Table S2). Only a single pellet was observed at 75 rpm with a mean diameter of 63.8 mm and 72.7 mm at inoculum densities of 20 and 40 mg L^{-1}, respectively, and therefore not included in the box and whisker plots. (E) Number of pellets in a 10 mL culture. Inoculum densities are on the dry weight basis. *Groups that share the same letters are considered statistically insignificant.

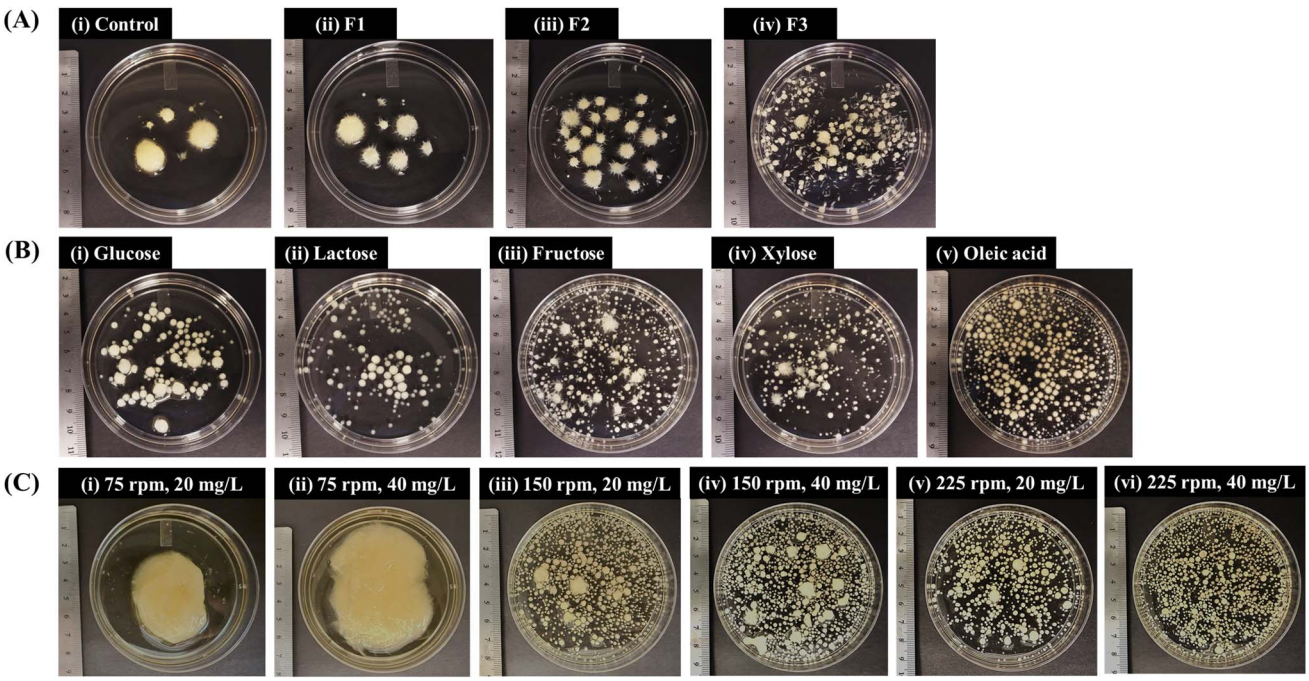

Fig. 5 Morphology of mycelial pellets under different (A) fragmentation levels. Control: no homogenization; F1: 3000 rpm, 5 s; F2: 5000 rpm, 10 s; and F3: 5000 rpm, 40 s. (B) Carbon sources at 3.6 g L^{-1} carbon loading harvested on day 8 and (C) inoculum densities and agitation rates.

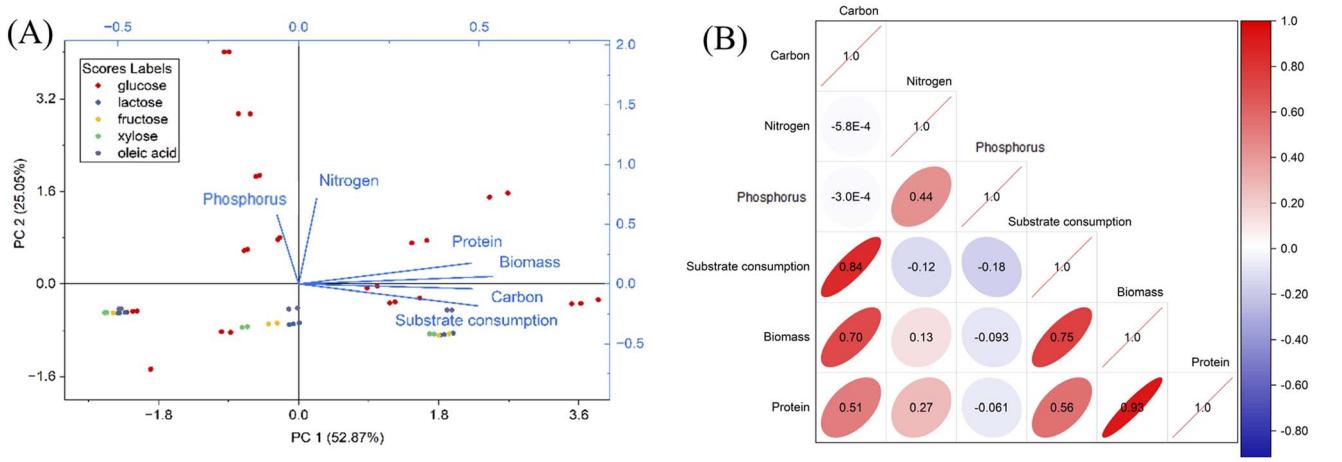

Fig. 6 (A) Biplot of principal component analysis and (B) Pearson's correlation matrix for the medium composition, carbon substrate consumption, and biomass and protein production from the submerged fermentation of *P. ostreatus*.

scale operations than large, loose, and heterogeneous mycelial clumps. The production of compact, uniform pellets is further supported by medium components such as glucose and oleic acid, which facilitate rounder pellet formation. In terms of primary recovery, these uniform pellet characteristics can facilitate more predictable filtration and dewatering rates. The compact nature of these pellets, combined with their smoother surface topography, reduces the entrapment of interstitial water within the fungal matrix, which can enhance the drying efficiency and reduce the energy footprint of moisture removal. Beyond harvesting, compact pellets provide a higher biomass density (as observed in Sections 3.1 and 3.3), which can improve the efficiency of mechanical cell disruption, ensuring the more consistent release of intracellular proteins. Furthermore, a standardized size distribution is critical for texturization processes such as extrusion, where a uniform raw material ensures consistent rheological behavior and heat transfer.[50] Therefore, this morphological control, governed by both physical and chemical parameters, is essential for ensuring consistent quality and streamlining the transition from fungal biomass to a structured food ingredient.

3.4. Principal component analysis

Principal component analysis (PCA) was conducted to study how the submerged fermentation parameters influence biomass and protein production and substrate consumption. Essentially, it reduces the dimensionality of the variables from the primary data into principal components and visualizes the contribution of each experimental factor to the variance. It was found that two major principal components, PC1 and PC2, describe 77.92% of the total variation, and a third principal component, PC3, provides an additional 12.7% of the variation (as shown in SI, Fig. S5). The loading plot (Fig. 6A) demonstrates the relative weight of each variable in PC1 and PC2, where all factors except for phosphorus loading contribute positively to PC1, and carbon loading and substrate consumption contribute negatively to PC2. The dots in the score plot represent the coordinates of individual data points in the new principal component space, with different carbon sources being distinguished by color. The results suggest that the majority of observations with glucose as the carbon source contribute positively to PC2, while observations with other carbon sources including lactose, fructose, xylose and oleic acid contribute negatively to PC2. Pearson's correlation analysis (Fig. 6B) was performed to understand the correlations among the variables. The analysis suggests that among the three key medium constituents including carbon, nitrogen and phosphorus loadings, carbon loading had a significantly positive correlation with the production of both biomass and protein, and substrate consumption. Meanwhile, nitrogen loading only had a strong positive correlation with protein production, rather than biomass. Phosphorus loading did not have any significant correlation with production or substrate consumption. These results are in good agreement with our previous findings.

4. Conclusions

The study herein developed a robust framework for enhancing mycelium-based protein production from *Pleurotus ostreatus* in submerged fermentation. The results highlight that precise control of the mycelial morphology can be achieved under specific inoculum fragmentation, agitation and inoculation density. The medium composition influences protein production, where a low C/N ratio (2.6) and a high C/P ratio (52.9) provided the highest protein content in mycelium (39.7% of biomass, d.b.). By integrating these findings with the appropriate agitation and inoculum density, the process achieved a maximum biomass titer of 12.9 g L^{-1}, with a productivity of 1.61 g L^{-1} day^{-1}. Furthermore, statistical analysis *via* PCA confirmed that the carbon loading strongly influenced both biomass and protein production, whereas the nitrogen loading was a significant driver primarily for protein synthesis, and phosphorus loading showed no significant correlation with either metric. This outlines a potential strategy for leveraging carbon and nitrogen-rich waste streams to optimize sustainable

co-production of mycelium biomass and protein at the industrial scale. Moreover, this work establishes oleic acid as a viable non-sugar carbon source, demonstrating the potential to improve the economic feasibility of large-scale production by valorizing lipid-rich waste streams (*e.g.*, used cooking oils or agricultural byproducts), thus avoiding competition with arable land and food crops required for conventional sugar feedstocks. This research advances the development of mycelium as a sustainable, food-grade vegan protein, offering a promising alternative to conventional animal-sourced protein. However, industrial-scale submerged fungal cultivation could be constrained by the high broth viscosity, limited oxygen transfer, and pellet clumping, which can obstruct/adhere to bioreactor components such as baffles, leading to process inconsistencies. Future research must address these scale-up dynamics by managing rheological behavior and maintaining morphological stability in large-scale bioreactors. Concurrently, further exploration can be directed towards deciphering the molecular-level mechanisms governing the variable performance of the species in response to the medium formulation.

Author contributions

Krishna Kalyani Sahoo: investigation, visualization, formal analysis, writing – original draft, writing – review & editing. Bruno Meireles Xavier: resources, supervision. Mohammad Afiq Hafiy Mohammad Taufiq: investigation, writing – original draft. Ke Wang: conceptualization, supervision, funding acquisition, formal analysis, writing – original draft, writing – review & editing.

Conflicts of interest

There are no conflicts to declare.

Data availability

The data supporting this article have been included as part of the supplementary information (SI). Supplementary information is available. See DOI: https://doi.org/10.1039/d5fb00752f.

Acknowledgements

The authors would like to thank the U.S. Department of Agriculture (USDA) Multistate S1075 program (The Science and Engineering for a Biobased Industry and Economy) seed grant for the funding support. The authors gratefully acknowledge the Cornell Biotechnology Resource Center (BRC) (Ithaca, NY, USA) for providing the genome sequencing services that are used to identify the fungal species. The authors also extend their sincere gratitude to Emile H. Punzalan from the Department of Food Science, Cornell University, for his invaluable assistance in operating the particle size analyzer and freeze dryer.

References

1 K. Smith, A. W. Watson, M. Lonnie, W. M. Peeters, D. Oonincx, N. Tsoutsoura, G. Simon-Miquel, K. Szepe, N. Cochetel, A. G. Pearson, O. C. Witard, A. M. Salter, M. Bennett and B. M. Corfe, *Eur. J. Nutr.*, 2024, **63**, 1425–1433.
2 U.S. Department of Agriculture, https://www.usda.gov/about-usda/news/press-releases/2022/06/01/usda-announces-framework-shoring-food-supply-chain-and-transforming-food-system-be-fairer-more, accessed on October 2025.
3 E. J. Derbyshire and J. Delange, *Front. Sustain. Food Syst.*, 2021, **5**, 581682.
4 K. K. Sahoo, S. Hao, J. M. I. Aquino and K. Wang, *Trends Food Sci. Technol.*, 2026, **170**, 105614.
5 M. E. Effiong, C. P. Umeokwochi, I. S. Afolabi and S. N. Chinedu, *Front. Nutr.*, 2024, **10**, 1279208.
6 A. Irshad, A. Tahir, S. Sharif, A. Khalid, S. Ali, A. Naz, H. Sadia, A. Ameen and D. P. Fulzele, *BioMed Res. Int.*, 2023, 2023.
7 G. Bakratsas, C. Tsoumanis, H. Stamatis and P. Katapodis, *Fermentation*, 2024, 10.
8 F. Ahmad Zakil, L. H. Xuan, N. Zaman, N. I. Alan, N. A. A. Salahutheen, M. S. M. Sueb and R. Isha, *Bioresour. Technol. Rep.*, 2022, **17**, 100873.
9 D. Tagkouli, A. Kaliora, G. Bekiaris, G. Koutrotsios, M. Christea, G. I. Zervakis and N. Kalogeropoulos, *Molecules*, 2020, **25**(17), 4015.
10 G. Bakratsas, K. Antoniadis, P. E. Athanasiou, P. Katapodis and H. Stamatis, *Biomass*, 2023, **4**, 1–22.
11 O. Datsomor, Q. Yan, L. Opoku-Mensah, G. Zhao and L. Miao, *Fermentation*, 2022, 8.
12 R. Rajput, B. Singh and M. Bashir Mir, in *Beta-Glucan: Sources, Properties and Applications*, 2025, ch. 11, pp. 189–205, DOI: 10.1007/978-3-031-95788-8_11.
13 H. El-Gendi, A. K. Saleh, R. Badierah, E. M. Redwan, Y. A. El-Maradny and E. M. El-Fakharany, *J. Fungi*, 2021, **8**(1), 23.
14 F. Humpenöder, B. L. Bodirsky, I. Weindl, H. Lotze-Campen, T. Linder and A. Popp, *Nature*, 2022, **605**, 90–96.
15 K. Majumder, B. Paul and R. Sundas, *J. Genet. Eng. Biotechnol.*, 2020, **18**(1), 47.
16 A. Musatti, E. Ficara, C. Mapelli, C. Sambusiti and M. Rollini, *J. Environ. Manage.*, 2017, **199**, 1–6.
17 V. Elisashvili, M. Penninckx, E. Kachlishvili, N. Tsiklauri, E. Metreveli, T. Kharziani and G. Kvesitadze, *Bioresour. Technol.*, 2008, **99**, 457–462.
18 M. M. Pascual, L. T. Herbert, M. Campos, V. Jurski, J. C. Painefilú and C. M. Luquet, *Innov. Food Sci. Emerg. Technol.*, 2025, **102**, 104021.
19 A. Hamza, M. P. Shankar, U. S. Chowdary, S. Ghanekar, S. Sahoo, C. V. Krishnaiah and D. S. Kumar, *Food Human.*, 2024, **2**, 100302.
20 G. M. Mascarin, P. S. Golo, C. de Souza Ribeiro-Silva, E. R. Muniz, A. de Oliveira Franco, N. N. Kobori and É. K. K. Fernandes, *Appl. Microbiol. Biotechnol.*, 2024, **108**(1), 451.

21 X. Zhang, H. Liu, M. Zhang, W. Chen and C. Wang, *J. Fungi*, 2023, **9**(11), 1120.
22 R. B. Nair, P. R. Lennartsson and M. J. Taherzadeh, *AMB Express*, 2016, **6**(1), 31.
23 G. Bakratsas, A. Polydera, O. Nilson, L. Kossatz, C. Xiros, P. Katapodis and H. Stamatis, *Sustain. Food Technol.*, 2023, **1**, 377–389.
24 X.-L. Li, X.-N. Qi, J.-C. Deng, P. Jiang, S.-Y. Wang, X.-L. Xue, Q.-H. Wang and X. Ren, *Foods*, 2025, **14**(4), 556.
25 V. Maini Rekdal, J. M. Villalobos-Escobedo, N. Rodriguez-Valeron, M. Olaizola Garcia, D. Prado Vásquez, A. Rosales, P. M. Sörensen, E. E. K. Baidoo, A. Calheiros de Carvalho, R. Riley, A. Lipzen, G. He, M. Yan, S. Haridas, C. Daum, Y. Yoshinaga, V. Ng, I. V. Grigoriev, R. Munk, C. H. Wijaya, L. Nuraida, I. Damayanti, P. Cruz-Morales and J. D. Keasling, *Nat. Microbiol.*, 2024, **9**, 2666–2683.
26 M. T. Nazir, A. M. Soufiani, J. A. Ferreira, T. Sar and M. J. Taherzadeh, *J. Chem. Technol. Biotechnol.*, 2022, **97**, 2626–2635.
27 S. Dzurendova, B. Zimmermann, V. Tafintseva, A. Kohler, D. Ekeberg and V. Shapaval, *Appl. Microbiol. Biotechnol.*, 2020, **104**, 8065–8076.
28 H. Liang, D.-W. Gao and Y.-G. Zeng, *Bioresour. Technol.*, 2012, **107**, 535–538.
29 M. Mohammadi, A. Zamani and K. Karimi, *Appl. Biochem. Biotechnol.*, 2013, **171**, 1465–1472.
30 Z. Wang, S. Li, H. Pan, Y. Li, X. Wang, H. Zhou and J. Shan, *J. Microbiol. Methods*, 2025, **238**, 107266.
31 C. Rosales-López, A. Vargas-López, M. Monge-Artavia and M. Rojas-Chaves, *Microorganisms*, 2022, **10**(7), 1404.
32 L. Cao, H. M. El Mashad, Z. Pan and R. Zhang, *Food Bioprocess Technol.*, 2025, **18**, 8735–8750.
33 G. E. Zharare, S. M. Kabanda and J. Z. Poku, *Sci. Hortic.*, 2010, **125**, 95–102.
34 H. Jeon, H. Son and K. Min, *Bio-protoc.*, 2023, **13**, e4889.
35 K. Shen, Y. Liu, L. Liu, A. W. Khan, N. Normakhamatov and Z. Wang, *Appl. Biochem. Biotechnol.*, 2024, **197**, 1534–1555.
36 G. L. Miller, *Anal. Chem.*, 1959, **31**, 426–428.
37 B. Wang, J. Chen, H. Li, F. Sun, Y. Li and G. Shi, *Bioprocess Biosyst. Eng.*, 2016, **40**, 45–53.
38 C. Falter and S. Reumann, *Mol. Plant Pathol.*, 2022, **23**, 781–794.
39 M. L. Hernández, M. D. Sicardo, A. Belaj and J. M. Martínez-Rivas, *Front. Plant Sci.*, 2021, **12**, 653997.
40 J. Shen, Y. Wang, P. Fan, L. Jiang, W. Zhuang, Y. Han and H. Zhang, *Colloids Surf., A Physicochem. Eng. Asp.*, 2019, **568**, 66–74.
41 S. Nakagame, H. Minagawa and N. Motegi, *Appl. Biochem. Biotechnol.*, 2022, **195**, 1085–1095.
42 F. Gallotti, C. Turchiuli and V. Lavelli, *J. Food Process. Eng.*, 2021, **45**, e13949.
43 J. Li, L. Lin, H. Li, C. Tian and Y. Ma, *Biotechnol. Biofuels*, 2014, **7**, 31.
44 C.-Y. Cheng, Y.-S. Wang, Z.-L. Wang and S. Bibi, *Foods*, 2023, **12**, 3477.
45 M. C. B. Tecson, C. Geluz, Y. Cruz and E. R. Greene, *Biochemistry*, 2025, **64**, 547–554.
46 Y. Cai, L. Zhai, X. Fang, K. Wu, Y. Liu, X. Cui, Y. Wang, Z. Yu, R. Ruan, T. Liu and Q. Zhang, *Biotechnol. Biofuels Bioprod.*, 2022, **15**(1), 102.
47 H. Wang, B. Hu, J. Liu, H. Qian, J. Xu and W. Zhang, *Bioprocess Biosyst. Eng.*, 2020, **43**, 1403–1414.
48 M. Takado, T. Komamura, T. Nishimura, I. Ohkubo, K. Ohuchi, T. Matsumoto and K. Takeda, *J. Biol. Chem.*, 2023, **299**(12), 105454.
49 D. Xing, X. Li, Y. Wang, S. Deng, C. Jin, Y. Zhao and L. Guo, *J. Water Proc. Eng.*, 2023, **51**, 103477.
50 T. A. L. Do, J. M. Hargreaves, B. Wolf, J. Hort and J. R. Mitchell, *J. Food Sci.*, 2007, **72**, E541.